

General Considerations Regarding Scattering of the MRI RF Field by Implanted Medical Devices

S. A. Mohsin¹, N. M. Sheikh¹, F. Mahmood¹ and W. Abbas²

1. Department of Electrical Engineering, University of Engineering and Technology, Lahore, Pakistan
syed_alimohsin@uet.edu.pk, omanchair@uet.edu.pk, fmahmood@uet.edu.pk
2. School of Electrical and Computer Engineering, Georgia Institute of Technology, Atlanta, GA, USA,
wabbas@gatech.edu

Abstract

The electromagnetic scattering problem posed by the interaction of the magnetic resonance imaging (MRI) RF field with a medical implant in tissue is explored. An exact formulation is computationally expensive since the domain includes all of the body tissue, the implant, the air region, and the surfaces of the RF coil conductors. It is shown that a division of the problem into two parts makes it more amenable to a numerical computation. In the first part, the RF field in the presence of body tissue only is found, and in the second part, the RF field that has already been computed is used as the incident field in the presence of the implant. Taking this incident field approximation into account, a domain simplification approximation is presented. A nonhomogeneous tissue layer surrounding the implant is considered and it is shown that then it is no longer necessary to integrate over all of the body tissue, and that the errors introduced due to this approximation are small enough to be considered as negligible. Numerical results validating the approximations are also presented.

1. Introduction

The radiofrequency (RF) field used in Magnetic Resonance Imaging (MRI) is scattered by implanted medical devices. The scattered field is concentrated in the tissue surrounding the implant and conduction currents will flow in this tissue resulting in potentially hazardous heating. Patients with medical implants can undergo MRI procedures and thus the scattering of the MRI RF field by medical implants merits a detailed investigation [1], [2], [3]. Transmission line theory can be used to find the current in an implant, and hence the scattered field [4], [5], [6], but this treatment is limited to thin linear structures implanted in homogeneous tissue. Numerical methods such as the method of moments (MoM), finite element method (FEM), or finite difference time domain (FDTD) can be employed, but for implants embedded in nonhomogeneous tissue the computational problem can be large and costly. Park et al [7] and Nyenhuis et al [8] used MoM to analyze scattering by deep brain stimulation (DBS) lead devices; the infinite and homogeneous tissue idealization was used to keep the computational problem small. Mohsin et al analyzed DBS leads near the air-tissue interface [9] and in partly nonhomogeneous tissue using FEM [10]. Ho et al [11] employed a commercial FDTD program to analyze metallic implants in nonhomogeneous tissue.

The present paper addresses the idealizations that have been used by previous researchers and suggests an approach to keep the scattering problem realistic as well as keeping the computational problem small. The remedies suggested do simplify the scattering problem to a large extent and are a better option than the previous approaches. First, the field that exists in the interior of the RF coil is found. This computation is done in the presence of body tissue with no implanted medical devices present. When one or more

implants are present, their loading effect on the MRI RF source is negligible. This is due to the fact that the scattered field produced by an implant decays very rapidly (tissue being a dissipative medium) and becomes negligible a short distance away from the implant. It follows that the RF field that exists inside body tissue in the absence of any implant can be used as the incident field when one or more implants are present. The formulation for the scattered field is further simplified so that the equivalent sources for the scattered field are over the implant volume and a small nonhomogeneous tissue region surrounding the implant. A numerical technique such as MoM can then be used with significantly less computational cost. The reduction in the size of the computational domain is a simplification of a general nature and is independent of the type of the implant.

2. Exact Formulation for the Total Field

Let S be the surface of the RF coil conductors (modeled as a perfect electric conductor, PEC) on which a surface current density \mathbf{K}_c exists, V^t is the volume occupied by tissue, V^i is the volume occupied by the implant (which may consist of more than one material). Then the total vector magnetic potential at any point is given by the integral formulation

$$\mathbf{A}(\mathbf{r}) = \frac{\mu_0}{4\pi} \left[\int_S \frac{\mathbf{K}_c e^{-jk|\mathbf{r}-\mathbf{r}'|}}{|\mathbf{r}-\mathbf{r}'|} dS' + \int_{V^t} \frac{\mathbf{J}_t e^{-jk|\mathbf{r}-\mathbf{r}'|}}{|\mathbf{r}-\mathbf{r}'|} dV' + \int_{V^i} \frac{\mathbf{J}_t e^{-jk|\mathbf{r}-\mathbf{r}'|}}{|\mathbf{r}-\mathbf{r}'|} dV' \right] \quad (1)$$

where \mathbf{r} and \mathbf{r}' are the observation and source points respectively, $k = \omega\sqrt{\mu_0\epsilon_0}$, and

$$\mathbf{J}_t = [\sigma + j\omega(\epsilon - \epsilon_0)] \mathbf{E} \quad (2a)$$

where σ and ε are conductivity and permittivity of body tissue (both are functions of position).

$$\mathbf{J}_I = [\sigma_I + j\omega(\varepsilon_I - \varepsilon_0)] \mathbf{E} \quad (2b)$$

where σ_I and ε_I are conductivity and permittivity of the implant materials (are functions of position). In (1), the volume integral over V^I is a general expression for any implant; for a particular implant, this expression will break up into a sum of volume integrals over the different parts of the implant (made of different materials). For any metal parts in the implant, the metal will be assumed to be a PEC and the volume integrals involving \mathbf{J}_I over the metallic parts, will be reduced to surface integrals involving surface current densities over the PEC surfaces. The electric field is given by:

$$\mathbf{E} = -\frac{j}{\omega \mu_0 \varepsilon_0} \vec{\nabla} (\vec{\nabla} \cdot \mathbf{A}) - j\omega \mathbf{A} \quad (3)$$

The wave equation for the total field \mathbf{E} is

$$\frac{1}{j\omega \mu_0} \nabla \times \nabla \times \mathbf{E} = -\mathbf{J} \quad (4)$$

where $\mathbf{J} = [\sigma + j\omega\varepsilon] \mathbf{E}$ in V^t , $\mathbf{J} = [\sigma_I + j\omega\varepsilon_I] \mathbf{E}$ in V^I , and $\mathbf{J} = \mathbf{J}_c$ represents the current density in the coil conductors (\mathbf{J}_c is limited to a few skin depths and $\mathbf{J}_c \rightarrow \mathbf{K}_c$ as $\sigma_c \rightarrow \infty$, that is, the skin depth approaches zero when the metal conductors of the coil are taken to be PEC; note that (1) incorporates this limiting case).

The exact formulation is over the entire interior of the RF coil and hence will use a lot of computational resources. A method such as MoM which uses fully populated matrices will be prohibitively expensive. FEM which uses sparse matrices is a better choice for numerically solving the exact formulation. We used a 64 GB RAM computational server for the solution by FEM.

3. Approximate Formulation for the Scattered Field

The various regions used in the formulation are shown in Figure 1. The implant V^I is surrounded by a finite nonhomogeneous tissue region V^0 with conductivity σ and permittivity ε , which are functions of position; the remaining tissue is homogeneous and extends to infinity in all directions (outwards) and has conductivity σ_b and permittivity ε_b . The extent of V^0 is based on the consideration that the scattered field decays very rapidly in tissue and is of an appreciable strength only in a tissue layer surrounding the implant surface. The thickness of V^0 can be chosen to be between 0.5 cm to 1 cm; the thicker the V^0

layer is, the more accurate the computation will be (but this will increase the number of unknowns to be solved for in MoM). Average body tissue constitutive parameters can be used as σ_b and ε_b . Typical values, as used in [7], are $\sigma_b = 0.27$ S/m and $\varepsilon_b = 77\varepsilon_0$. Note that the outlying tissue σ_b , ε_b does not affect the scattered field to a large degree. The incident field $\{\mathbf{E}^i, \mathbf{H}^i\}$ used here is the field that exists in the interior of the RF coil in the presence of body tissue but in the absence of any implant. The computation of $\{\mathbf{E}^i, \mathbf{H}^i\}$ is done only once for a particular position of the landmark (center of the RF coil) relative to the body tissue, [12], [13], and then the computed $\{\mathbf{E}^i, \mathbf{H}^i\}$ can be used for different implants by employing the formulation presented here.

The incident field $(\mathbf{E}^i, \mathbf{H}^i)$ satisfies

$$\left. \begin{aligned} \text{In outlying tissue :} \\ \vec{\nabla} \times \mathbf{H}^i &= \sigma_b \mathbf{E}^i + j\omega \varepsilon_b \mathbf{E}^i \\ \vec{\nabla} \times \mathbf{E}^i &= -j\omega \mu_0 \mathbf{H}^i \end{aligned} \right\} \dots\dots(5a)$$

$$\left. \begin{aligned} \text{In } V^0 \cup V^I \text{ (i.e., in tissue surrounding} \\ \text{the implant, and in the volume occupied} \\ \text{by the implant) : } \vec{\nabla} \times \mathbf{H}^i &= \sigma \mathbf{E}^i + j\omega \varepsilon \mathbf{E}^i \\ \vec{\nabla} \times \mathbf{E}^i &= -j\omega \mu_0 \mathbf{H}^i \end{aligned} \right\} \dots\dots(5b)$$

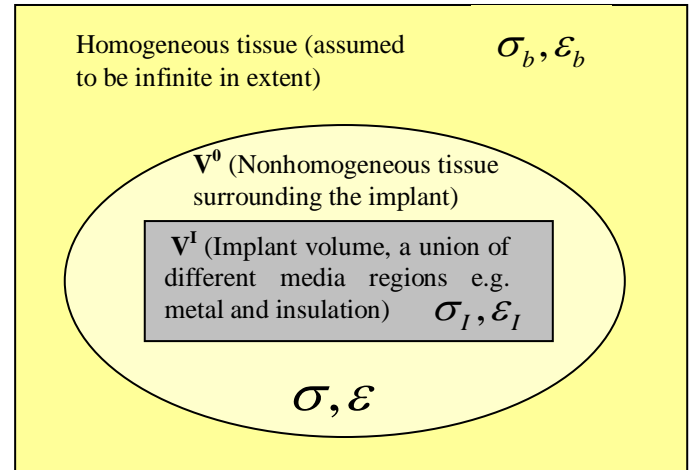


Fig. 1 Regions used in the domain simplification. The incident field used as the excitation here is that which exists in body tissue in the absence of any implant. The magnetic permeability is μ_0 in all regions.

The total field (\mathbf{E}, \mathbf{H}) in the presence of the implant satisfies

$$\left. \begin{aligned} \text{In outlying tissue } \vec{\nabla} \times \mathbf{H} &= \sigma_b \mathbf{E} + j\omega \varepsilon_b \mathbf{E} \\ : \vec{\nabla} \times \mathbf{E} &= -j\omega \mu_0 \mathbf{H} \end{aligned} \right\} \dots\dots(6a)$$

$$\left. \begin{aligned} \text{In inlying tissue } V^0 \quad \vec{\nabla} \times \mathbf{H} &= \sigma \mathbf{E} + j\omega \varepsilon \mathbf{E} \\ \vec{\nabla} \times \mathbf{E} &= -j\omega \mu_o \mathbf{H} \end{aligned} \right\} \dots(6b)$$

where σ and ε are functions of position in the nonhomogeneous tissue region V^0 .

$$\left. \begin{aligned} \text{In the implant } V^I \quad \vec{\nabla} \times \mathbf{H} &= \sigma_I \mathbf{E} + j\omega \varepsilon_I \mathbf{E} \\ : \quad \vec{\nabla} \times \mathbf{E} &= -j\omega \mu_o \mathbf{H} \end{aligned} \right\} \dots(6c)$$

where σ_I and ε_I take different values in different parts of the implant.

Therefore the scattered field $(\mathbf{E}^s, \mathbf{H}^s) = (\mathbf{E} - \mathbf{E}^i, \mathbf{H} - \mathbf{H}^i)$ satisfies:

$$\left. \begin{aligned} \text{In outlying tissue } \vec{\nabla} \times \mathbf{H}^s &= \sigma_b \mathbf{E}^s + j\omega \varepsilon_b \mathbf{E}^s \\ \vec{\nabla} \times \mathbf{E}^s &= -j\omega \mu_o \mathbf{H}^s \end{aligned} \right\} \dots(7a)$$

In inlying tissue V^0

$$\left. \begin{aligned} \vec{\nabla} \times \mathbf{H}^s &= \sigma \mathbf{E}^s + j\omega \varepsilon \mathbf{E}^s \\ &= \mathbf{J}_I + (\sigma_b + j\omega \varepsilon_b) \mathbf{E}^s \\ \vec{\nabla} \times \mathbf{E}^s &= -j\omega \mu_o \mathbf{H}^s \end{aligned} \right\} \dots(7b)$$

$$\text{where } \mathbf{J}_I = [(\sigma - \sigma_b) + j\omega(\varepsilon - \varepsilon_b)] \mathbf{E}^s$$

In the Implant V^I :

$$\left. \begin{aligned} \vec{\nabla} \times \mathbf{H}^s &= \\ \sigma_I \mathbf{E} + j\omega \varepsilon_I \mathbf{E} - \sigma \mathbf{E}^i - j\omega \varepsilon \mathbf{E}^i \\ &= \mathbf{J}_I + (\sigma_b + j\omega \varepsilon_b) \mathbf{E}^s \\ \vec{\nabla} \times \mathbf{E}^s &= -j\omega \mu_o \mathbf{H}^s \end{aligned} \right\} \dots(7c)$$

$$\text{where } \mathbf{J}_I = [(\sigma_I - \sigma_b) + j\omega(\varepsilon_I - \varepsilon_b)] \mathbf{E}^s + [(\sigma_I - \sigma) + j\omega(\varepsilon_I - \varepsilon)] \mathbf{E}^i$$

Defining a vector magnetic potential \mathbf{A}^s and a scalar electric potential ϕ^s by

$$\mu_o \mathbf{H}^s = \vec{\nabla} \times \mathbf{A}^s \quad (8a)$$

$$\mathbf{E}^s + \vec{\nabla} \phi^s = -j\omega \mathbf{A}^s \quad (8b)$$

$$\vec{\nabla} \cdot \mathbf{A}^s = -j\omega \mu_o \left(\varepsilon_b - \frac{j\sigma_b}{\omega} \right) \phi^s \quad (8c)$$

We derive the wave equations

$$\nabla^2 \mathbf{A}^s + \omega^2 \mu_o \left(\varepsilon_b - \frac{j\sigma_b}{\omega} \right) \mathbf{A}^s = -\mu_o \mathbf{J} \quad (9a)$$

$$\nabla^2 \phi^s + \omega^2 \mu_o \left(\varepsilon_b - \frac{j\sigma_b}{\omega} \right) \phi^s = \frac{-\rho_v}{\left(\varepsilon_b - \frac{j\sigma_b}{\omega} \right)} \quad (9b)$$

where

$$\rho_v = \frac{j}{\omega} (\vec{\nabla} \cdot \mathbf{J}) \quad \text{and}$$

$$\mathbf{J}(\mathbf{r}) = \mathbf{J}_I(\mathbf{r})$$

$$= [(\sigma_I - \sigma_b) + j\omega(\varepsilon_I - \varepsilon_b)] \mathbf{E}^s$$

$$+ [(\sigma_I - \sigma) + j\omega(\varepsilon_I - \varepsilon)] \mathbf{E}^i, \quad \mathbf{r} \in V^I \quad (10a)$$

$$\mathbf{J}(\mathbf{r}) = \mathbf{J}_I(\mathbf{r}) = [(\sigma - \sigma_b) + j\omega(\varepsilon - \varepsilon_b)] \mathbf{E}^s, \quad \mathbf{r} \in V^0 \quad (10b)$$

$$\mathbf{J}(\mathbf{r}) = 0 \quad \text{in outlying tissue} \quad (10c)$$

where \mathbf{r} is the position vector of a point. From (9a) and (10abc) we find the formulation

$$\begin{aligned} \mathbf{A}^s(\mathbf{r}) &= \frac{\mu_o}{4\pi} \int_{V^0} \frac{\mathbf{J}_I e^{-jk|\mathbf{r}-\mathbf{r}'|}}{|\mathbf{r}-\mathbf{r}'|} dV' \\ &+ \frac{\mu_o}{4\pi} \int_{V^I} \frac{\mathbf{J}_I e^{e^{-jk|\mathbf{r}-\mathbf{r}'|}}}{|\mathbf{r}-\mathbf{r}'|} dV' \quad \dots\dots\dots(11) \end{aligned}$$

where \mathbf{r} and \mathbf{r}' are the (field) observation and source

points respectively and $k = \omega \sqrt{\mu_o \left(\varepsilon_b - \frac{j\sigma_b}{\omega} \right)}$. In (11),

the volume integral over V^I will be a sum of, volume integrals over different parts of the implants (having different $(\sigma_I, \varepsilon_I)_i$); volume integrals over metallic parts will reduce to surface integrals over PEC surfaces. The scattered field is

$$\mathbf{E}^s = -\frac{j}{\omega \mu_o} \frac{\vec{\nabla} (\vec{\nabla} \cdot \mathbf{A}^s)}{(\varepsilon_b - j\sigma_b/\omega)} - j\omega \mathbf{A}^s \quad (12)$$

When the nonhomogeneous tissue region V^0 is replaced by the background medium, we have $\sigma = \sigma_b$ and $\varepsilon = \varepsilon_b$ so that $\mathbf{J}_I = 0$ and (11) becomes

$$\mathbf{A}^s(\mathbf{r}) = \frac{\mu_o}{4\pi} \int_{V^I} \frac{\mathbf{J}_I e^{-jk|\mathbf{r}-\mathbf{r}'|}}{|\mathbf{r}-\mathbf{r}'|} dV' \quad \dots\dots\dots(13)$$

where $\mathbf{J}_I = [(\sigma_I - \sigma_b) + j\omega(\epsilon_I - \epsilon_b)](\mathbf{E}^s + \mathbf{E}^i)$. This (simplest) homogeneous and infinite medium assumption has been used in [7], [14] and [15] for the analysis of lead implants. It seems appropriate that instead of replacing all of V^0 by the background medium at least a small V^0 should be used, say 0.5 cm to 1 cm, surrounding the implant. This will increase the computational cost somewhat (not as much as using a larger, say 3 to 5cm, V^0) but that will be much better than using no nonhomogeneity at all.

4. Results and Discussion

The domain simplification approach presented in the previous section does not depend on the type of the implant (i.e., its geometry and composition) since the formulations (6c) thru (11) are perfectly general; the approach does not restrict itself to a particular type of implant: note that the constitutive parameters of the implant σ_I, ϵ_I are taken to be arbitrary functions of position; no specific space distribution is specified. For validation, therefore, we can choose any implant. Our purpose is to compare the results of our computational approaches, not to evaluate and study the scattering and the consequent MRI induced heating behavior of a particular type of implant per se. We consider a model lead implant proposed in a FDA standard [16], since measurement and simulation studies of this implant are commonly available [13] [15]. The implant consists of a solid metal cylinder 1.6 mm in diameter and 20 cm long. It is sheathed in an 18 cm long insulation cover having an outer dia of 2.5 mm, so that each of the bare ends (electrodes) is 1 cm long. The metal is modeled as a PEC; the relative permittivity of the insulation is 3.0. The lead is implanted in nonhomogeneous tissue consisting of alternate sections of muscle and fat so that the central part of the implant (lengthwise) is embedded in muscle. The relative permittivity, ϵ_r , and conductivity, σ , of muscle tissue are 80 and 0.5 S/m respectively ; for fat tissue the respective values are 6.5 and 0.0353 S/m. The implant and the tissue in which it is implanted is positioned such that the center of the MRI birdcage coil (landmark) coincides with the center (lengthwise) of the implant. The strength of the MRI system is 1.5 Tesla which corresponds to a RF of 63.86 MHz. The applied MRI input power is such that the background SAR in tissue at the landmark is 2.5 W/kg. The first computation is for an exact formulation of the total field as described in Section II (without recourse to the domain simplification shown in Fig. 1). The finite element method (FEM), [17], is used to find the total field. Comsol Multiphysics has been used as the FEM based partial differential equation solver. The computational domain is discretized using a large number of elements (approximately 3×10^5) to achieve a high degree of accuracy. At a MRI RF of 63.86 MHz the wavelength of the RF field in air is 4.7m. Wavelengths in body tissue are from 42.6 cm (in muscle with $\sigma = 0.5$ S/m, $\epsilon_r = 80$) to 154.6 cm (in fat with $\sigma = 0.0353$ S/m, $\epsilon_r =$

6.5). The size of the finite elements used is $\lambda/10$ or smaller, where λ is the wavelength. The computation time for the scattered field was about ten hours on a 64GB RAM multicore computational server. Fig. 2 shows the current in the implant and Fig. 3 shows the spatial electric field distribution in the tissue surrounding the electrodes at the ends of the implant. The bioheat equation, [8], [9], is solved using FEM to find the induced temperature rise in the tissue surrounding the implant. The results obtained are shown in Figs. 4 and 5.

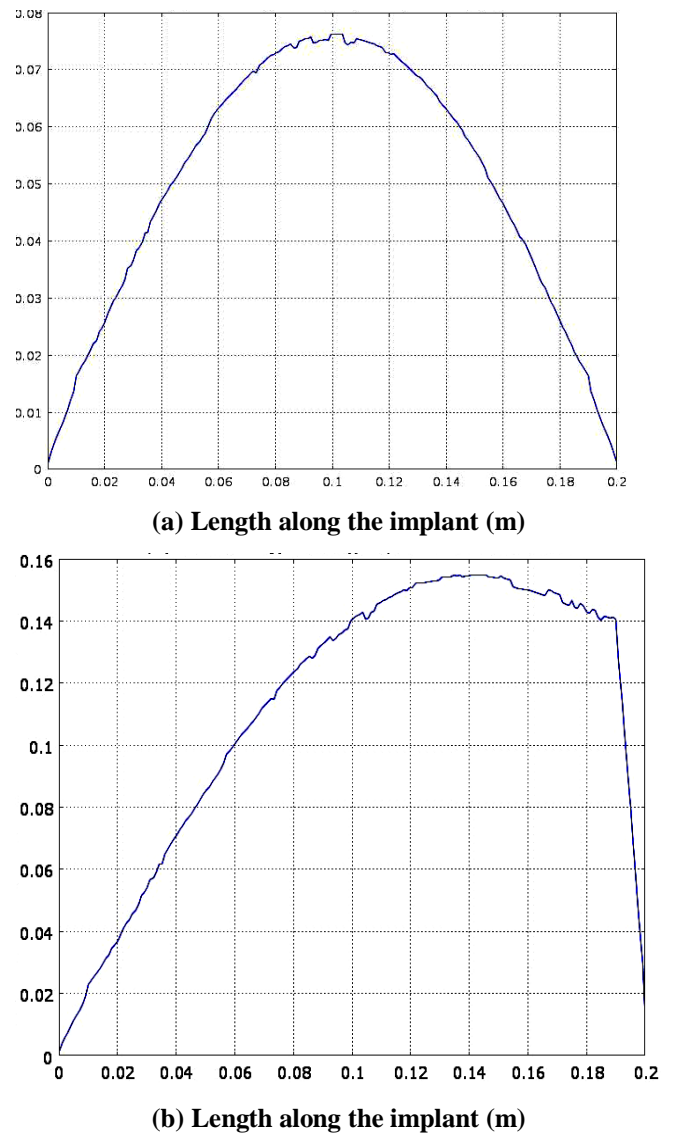
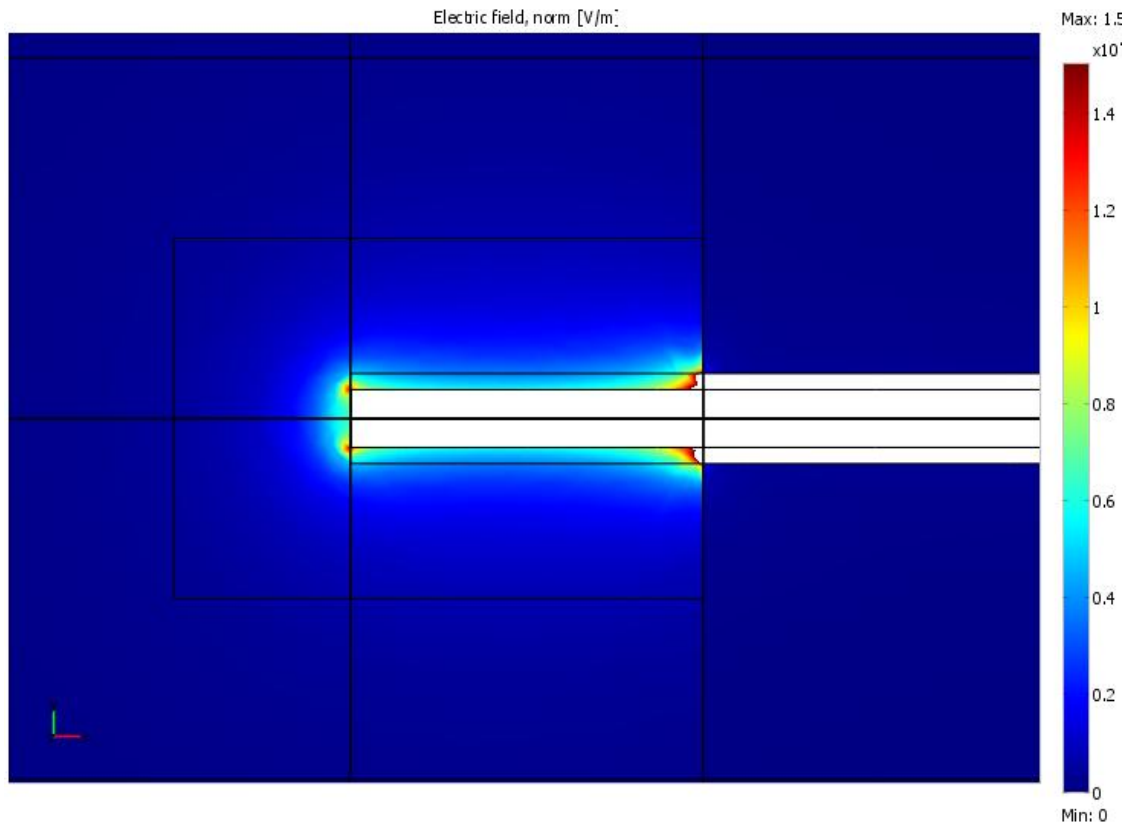
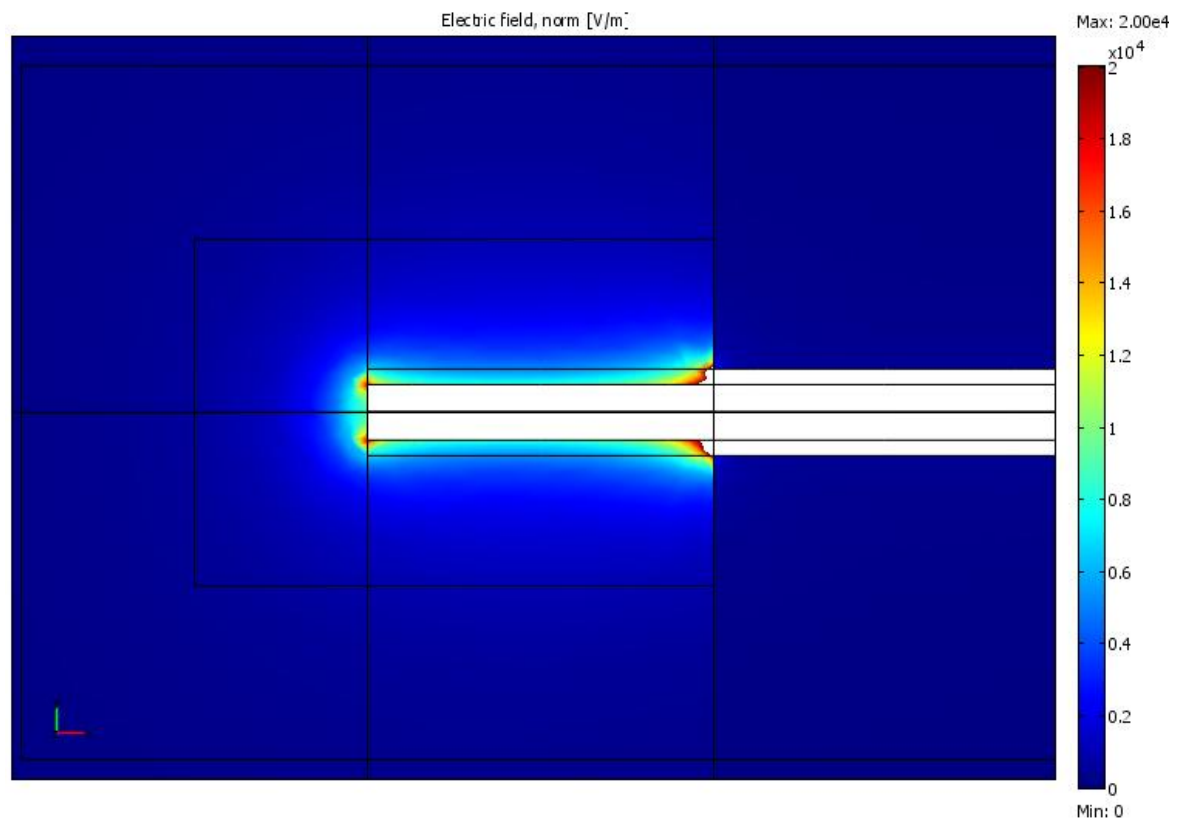


Fig. 2 Magnitude of the current in the implant (in amperes) is along the vertical axis. (a) both ends in fat tissue (b) left end in fat, right end in muscle tissue

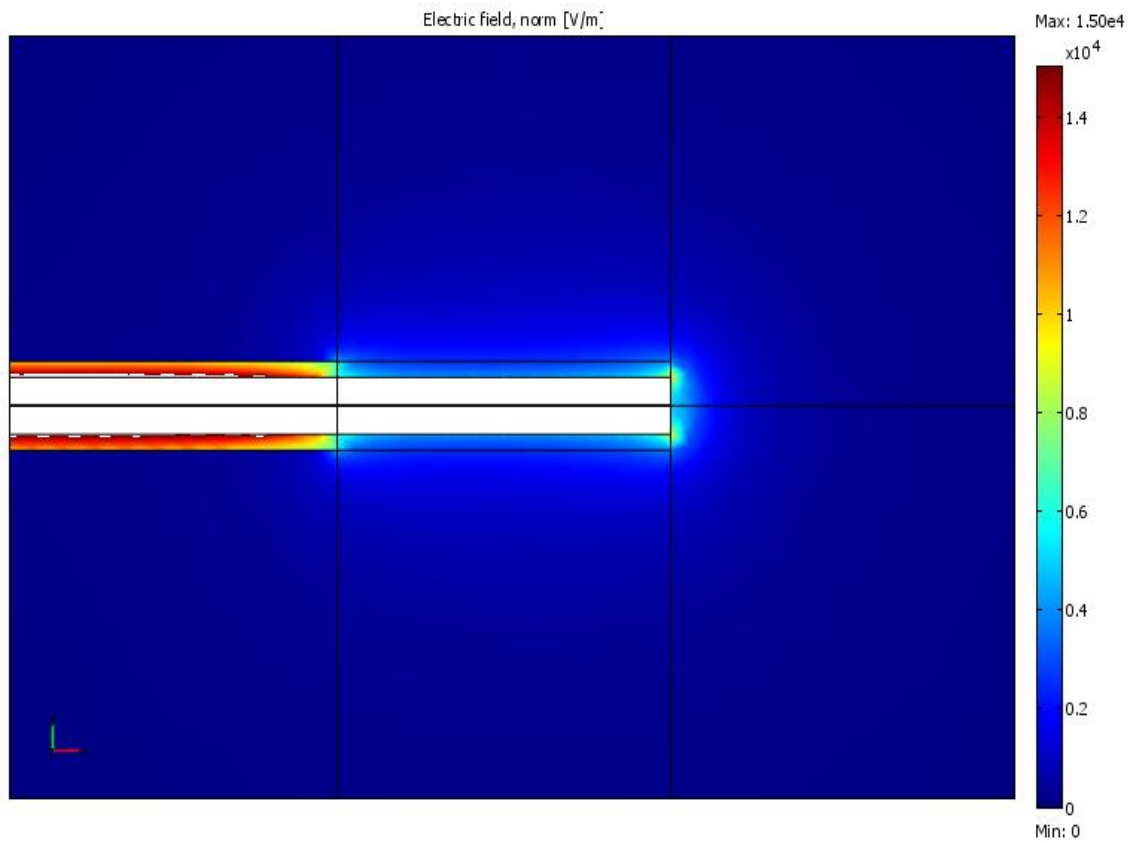
A second computation is carried out using the approximate formulation outlined in Section III of this paper (illustrated in in Fig. 1). MoM, as outlined in [18], is used for the numerical computation. The computation time was about three hours on the same server machine. The overall shape of the graphs for FEM and MoM is similar. The peak value of the current along the implant and the spatially



(a)

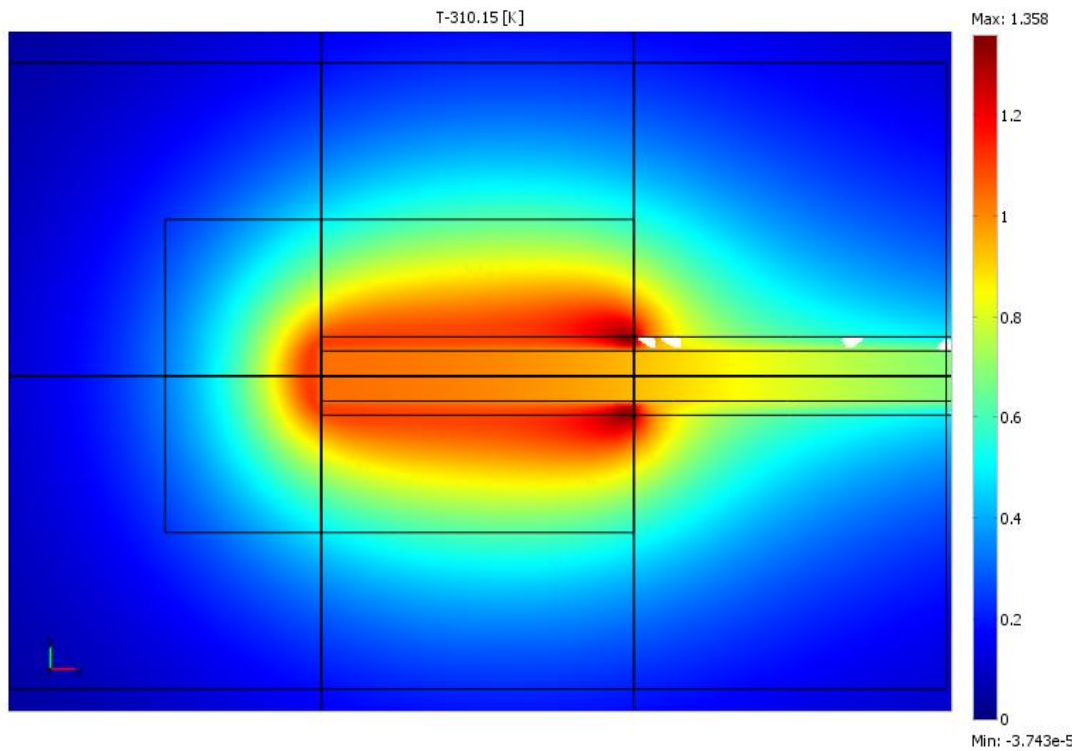


(b) (i)

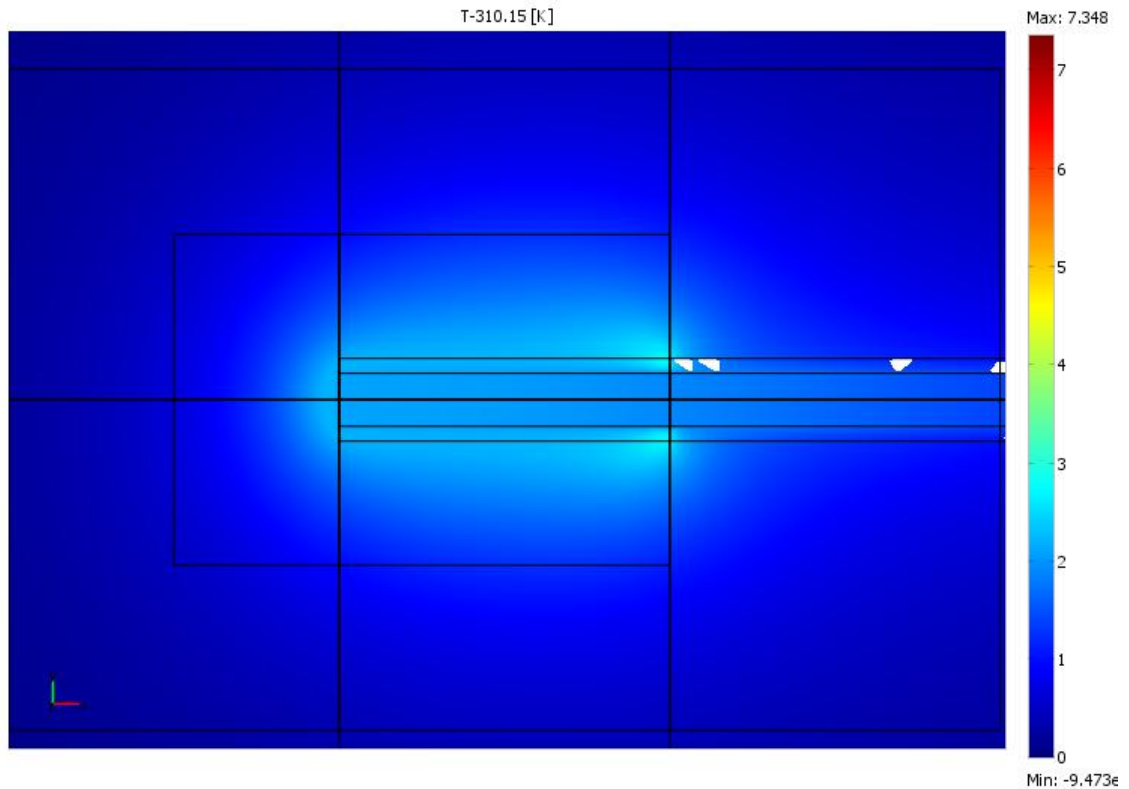


(b) (ii)

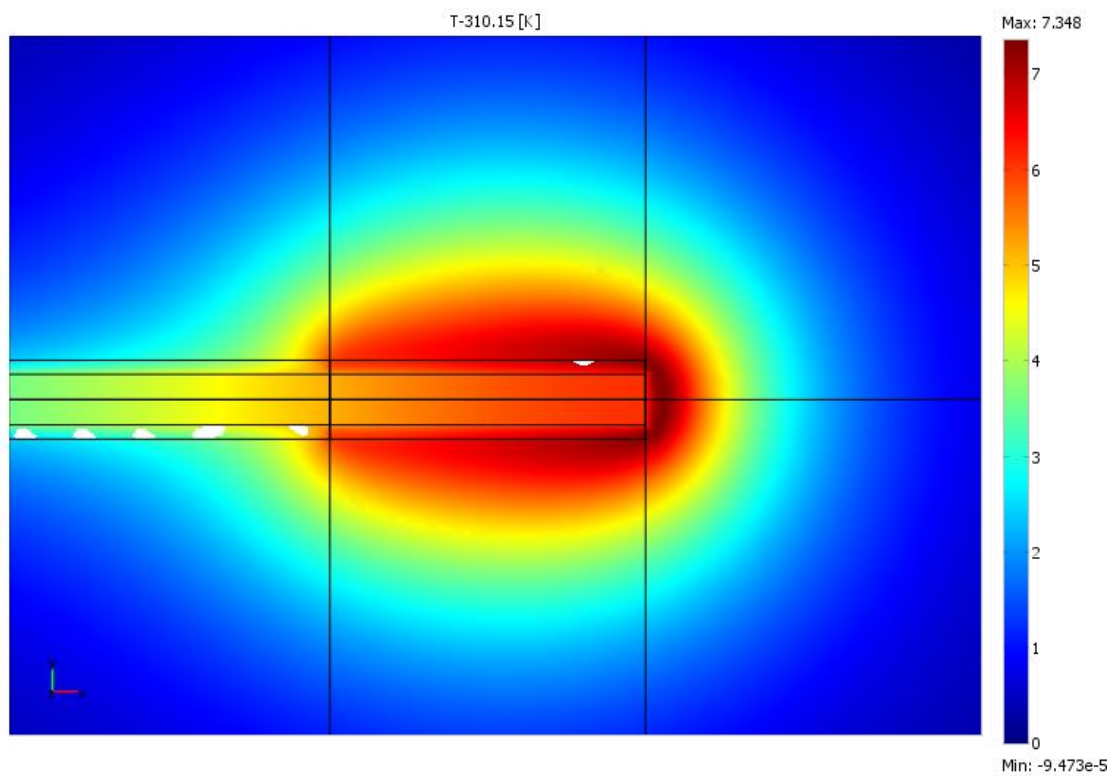
Fig. 3 Spatial electric field distributions in the tissue surrounding the electrodes. (Scale: Each square is 1cm \times 1cm) (a) both ends in fat tissue; only one electrode is shown (the distribution at the other end is the same). (b) left electrode is in fat tissue, right electrode is in muscle tissue: (i) left electrode (ii) right electrode



(a)



(b) (i)



(b) (ii)

Fig. 4 Spatial temperature rise distributions around the electrodes after six minutes of continuous application of MRI input power. (Scale: Each square is $1\text{cm} \times 1\text{cm}$). Composition of the surrounding tissue is as for Fig. 3: (i) left electrode (ii) right electrode

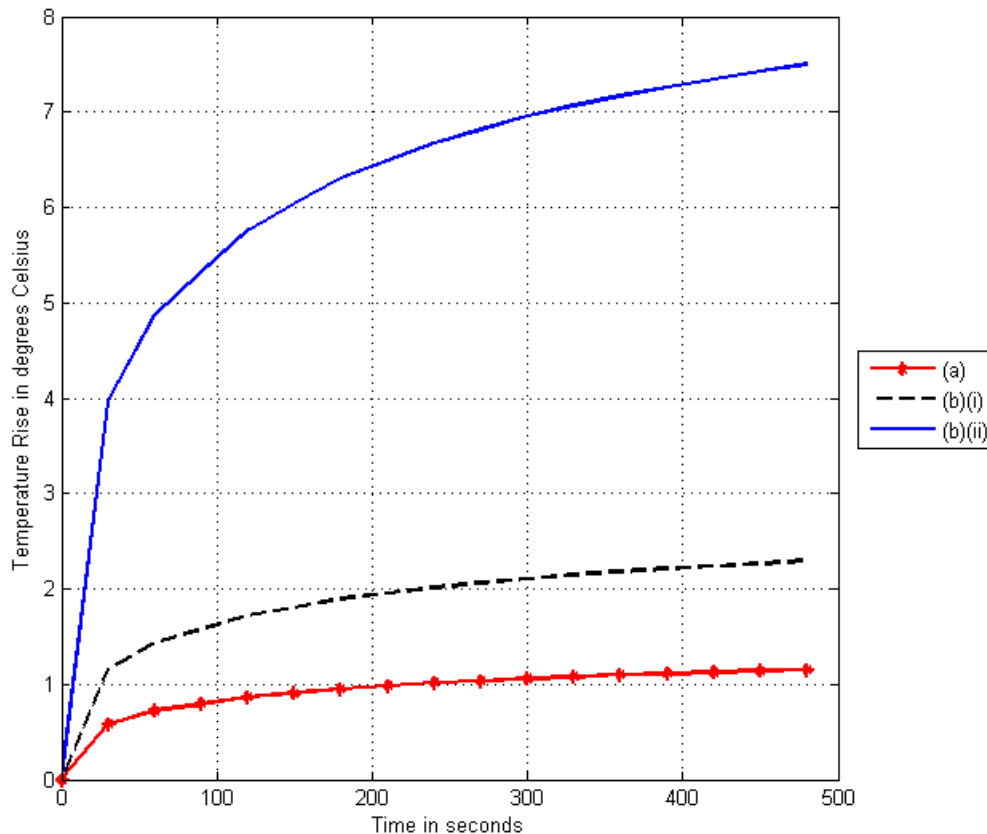


Fig. 5 Temperature rise versus time plots at a point in tissue 1.3 mm radially away from the cylindrical central axis of the implant and 0.5 mm inwards from the distal end. (a) and (b) in the legend refer to the composition of tissue as in Fig. 3: (i) refers to the left electrode, and (ii) to the right electrode

maximum electric field value obtained from the exact formulation, as shown in Figs. 2 and 3, are about 97 % of the values obtained from the approximate formulation. For the exact formulation, the temperature rises after 6 minutes at a point in tissue near the implant are found to be 1.1°C, 2.2°C, and 7.2°C (see Fig, 5) which compare well with 1.1°C, 2.3°C, and 7.4°C respectively, obtained for the approximate formulation.

5. Conclusions

An approximate scattering formulation is presented in which the loading effect of the implant on the MRI sources is neglected and only the nonhomogeneity of tissue in the proximity of the implant is considered. Computations have been carried out to validate the simplifications made in the scattering problem. The results obtained for the exact and approximate formulations agree well with each other and with computations and measurements by other researchers, [13] [15], made on this model implant.

Acknowledgements

The first author wishes to acknowledge the cooperation of the MRI RF research group in the Department of Electrical Engineering, Purdue University, West Lafayette, IN, U.S.A. during his stay as a Visiting Research Scientist there.

REFERENCES

- [1] A.R. Rezai, D. Finnelli, J. A. Nyenhuis, G. Hrdlicka, J. Tkach, A. Sharan, P. Rugieri, P. H Stypulkowski, and F. G. Shellock, "Neurostimulation Systems for Deep Brain Stimulation: In Vitro Evaluation of Magnetic Resonance Imaging-Related Heating at 1.5 Tesla," J Magn. Reson. Imaging, Vol. 15, pp. 241-250, 2002.
- [2] M. Bock, R. Umatham, S. Zuehlsdorff, S. Volz, C. Fink, P. Hallscheidt, H. Zimmermann, W. Nitz and W. Semmler, "Interventional Magnetic Resonance Imaging: an Alternative to Image Guidance with Ionizing Radiation", Radiation Protection Dosimetry, Vol. 117, No. 1-3, pp. 74-78, February 2006.
- [3] T. M. Peters., "Image-Guidance for Surgical Procedures", Phys. Med. Biol., Vol. 51, No. 14, pp. R505-R540, July 2006.
- [4] W. R. Nitz, A. Oppelt, W. Renz, C. Manke, M. Lenhart, and J. Link, "On the Heating of Linear Conductive Structures as Guide Wires and Catheters in Interventional MRI," J. Magn. Reson. Imag., Vol. 13, pp. 105-113, 2001.
- [5] R. P. King , "Antennas in material media near boundaries with application to communication and geophysical exploration, Part I: The bare metal dipole," IEEE Transactions on Antennas and

- Propagation, Volume 34, Issue 4, pp. 483 – 489, April 1986.
- [6] R. P. King, “Antennas in material media near boundaries with application to communication and geophysical exploration, Part II: The terminated insulated antenna,” *IEEE Transactions on Antennas and Propagation*, Volume 34, Issue 4, pp. 490 – 496, April 1986.
- [7] S.M. Park, R. Kamondetdacha, A. Amjad, and J. A. Nyenhuis, “MRI safety: RF induced heating on straight wires,” *IEEE Trans. Magn.*, Vol. 41, No. 10, pp. 4197-4199, Oct. 2005.
- [8] J. A. Nyenhuis, S.M. Park, R. Kamondetdacha, A. Amjad, F.G. Shellock, and A. Rezai, “MRI and Implanted Medical Devices: Basic Interactions With an Emphasis on Heating,” *IEEE Trans. Device and Materials Reliability*, Vol. 5, No. 3, Sep. 2005.
- [9] Mohsin, S. A., N. M. Sheikh, U. Saeed, “MRI-induced heating of deep brain stimulation leads,” *Phys. Med. Biol.*, 5745-5756, 2008
- [10] Mohsin, S. A., N. M. Sheikh, U. Saeed, “MRI induced heating of deep brain stimulation leads: effect of the air-tissue interface,” *Progress In Electromagnetics Research*, PIER 83, 81–91, 2008.
- [11] H. S. Ho, “Safety of Metallic Implants in Magnetic Resonance Imaging,” *J. Magn. Reson. Imag.*, Vol. 14, pp. 472-474, 2001.
- [12] A. Amjad, R. Kamondetdacha, A.V. Kildishev, S. M. Park, J. A. Nyenhuis, “Power deposition inside a phantom for testing of MRI heating,” *IEEE Trans Magn* 2005, 41:4185–4187.
- [13] A. Amjad, “Specific Absorption Rate during Magnetic Resonance Imaging,” Ph.D Thesis, Purdue University, 2007.
- [14] S. M. Park, “MRI Safety: Radiofrequency Field Induced Heating of Implanted Medical Devices,” Ph. D Thesis, Purdue University, 2006.
- [15] Sung-Min Park, Rungkiet Kamondetdacha, and John A. Nyenhuis, “Calculation of MRI-Induced Heating of an Implanted Medical Lead Wire With an Electric Field Transfer Function”, *Journal of Magnetic Resonance Imaging* 26:1278–1285, 2007.
- [16] W. Kainz, SAR intercomparison protocol for 1.5 T MR systems draft, U.S. Food and Drug Administration, Center for Devices and Radiological Health, Office of Science and Engineering Laboratories, 2006.
- [17] John L. Volakis, Arindam Chatterjee, and Leo C. Kempel, “Finite Element Method for Electromagnetics,” *The IEEE/OUP Series on Electromagnetic Wave Theory*.
- [18] Roger F. Harrington, “Field Computation by Moment Methods,” *Wiley-Interscience and IEEE Press Series on Electromagnetic Wave Theory*, 1993.